Completed Three-Dimensional Model of Human Coagulation Factor Va. Molecular Dynamics Simulations and Structural Analyses†

Tivadar Orban,‡ Michael Kalafatis,‡,§ and Valentin Gogonea*,‡,||

Department of Chemistry, Cleveland State University, and Departments of Molecular Cardiology and Immunology, Lerner Research Institute, Cleveland Clinic Foundation, 9500 Euclid Avenue, Cleveland, Ohio 44195

Received May 13, 2005; Revised Manuscript Received July 28, 2005

ABSTRACT: Factor Va is the critical cofactor for prothrombinase assembly required for timely and efficient prothrombin activation. In the absence of a complete crystal structure for the cofactor, Pellequer et al. [(2000) *Thromb. Haemostasis 84*, 849−857] proposed an incomplete homology model of factor Va (it lacks 46 amino acids from the carboxyl terminus of the heavy chain), which is a static model in a vacuum. A recently published X-ray structure of activated protein C (APC) inactivated bovine factor Va_i (without the A2 domain) suggests a completely new arrangement of the C1 and C2 domains as compared with the previously published structure of the recombinant C1 and C2 domains. Our aims were (a) to exchange the C1 and C2 domains of the homology model with the modified bovine C1 and C2 domains using the X-ray structure as a template, (b) to determine by computation the three-dimensional model for the carboxyl-terminal peptide of the factor Va heavy chain (Ser^{664}−Arg^{709}) and incorporate it into the incomplete model, (c) to obtain a complete model of the cofactor folded in solution that might account for its physiological functions and interactions with other components of prothrombinase, and (d) to use the model in order to understand the mechanism of factor Va inactivation by APC. In the first step a sequence alignment of the human and bovine C1 and C2 domains was performed followed by amino acid changes in the three-dimensional structure where the sequences were not identical. The new model of the C1 and C2 domains was then attached to the homology model. The analysis of the MD simulation data revealed that several domains of the cofactor were significantly displaced during simulation. Using our completed model of human factor Va, we are also demonstrating for the first time that cleavage of membrane-bound normal factor Va as well as membrane-bound factor V^{LEIDEN} by APC at Arg^{306} is required for the dissociation of the A2 domain from the rest of the molecule. Thus, differences in the inactivation rates of the two cofactor molecules are due to differences in the rate of cleavage at Arg^{306}. The data demonstrate that our model represents the foundation for the establishment of a complete prothrombinase complex model, which might be successful in describing accurately the ternary protein−protein interaction and thus accounts for experimental observations.

Factor Va is the cofactor required for prothrombinase complex assembly and function (*1*). Following vascular injury, the active cofactor combines with factor Xa, on a membrane surface in the presence of Ca^{2+} ions (*2*), and the complex will readily activate prothrombin to thrombin (*3*). Thrombin, which has multiple functions, rapidly activates platelets, converts fibrinogen to fibrin, and activates factor XIII. Cross-linked fibrin and activated platelets will produce the insoluble plug which is necessary to stop blood leaking outside the vasculature (*4*). Factor Xa alone converts prothrombin to thrombin with a rate of activation which is 5 orders of magnitude lower than the rate of the reaction catalyzed by factor Xa bound to factor Va on a negatively charged membrane surface in the presence of Ca^{2+} ions (*3*). The increase in the catalytic efficiency of prothrombinase when compared to the activation of prothrombin by factor Xa alone appears to result from a decrease in the K_m representing higher local substrate concentrations and an increase in the k_{cat} of the enzyme corresponding to more efficient catalysis because of the altered pathway for prothrombin cleavage and activation (*5*−*7*). Thus, incorporation of factor Va into prothrombinase and its interaction with the components of the ternary complex are requirements for normal hemostasis.

Factor V circulates in plasma as an inactive procofactor with high molecular weight (M_r 330000). The procofactor is activated to factor Va by α-thrombin (*2*). Factor Va is composed of a heavy chain (M_r 105000, Ala^1−Arg^{709}), containing the A1 and A2 domains (*8*), and a light chain (M_r 74000, Ser^{1546}−Tyr^{2196}), containing the A3, C1, and C2 domains noncovalently associated in the presence of divalent metal ions. While both chains of factor Va are required for the interaction with factor Xa, only the heavy chain of the cofactor binds prothrombin (*9*−*12*). Cleavage of factor Va

† This work was supported by funds from the Department of Energy (Grant DE-FG02-03ER15462) and National Institutes of Health (Grant 1R15GM070469-01) (to V.G.) and by Established Investigator Award 0040100N from the American Heart Association and Grant 1R01HL-73343 from the National Institutes of Health (to M.K.).

* To whom correspondence should be addressed at the Department of Chemistry, Cleveland State University. Tel: (216) 875-9717. E-mail: v.gogonea@csuohio.edu.

‡ Department of Chemistry, Cleveland State University.

§ Department of Molecular Cardiology, Cleveland Clinic Foundation.

|| Department of Immunology, Cleveland Clinic Foundation.

10.1021/bi050891t CCC: $30.25
Published on Web 09/10/2005

by activated protein C (APC)[1] at Arg^{506}/Arg^{679} results in decreased affinity of the molecule for factor Xa and the elimination of its interaction with prothrombin (*10*, *13*, *14*). Subsequent cleavage of the membrane-bound cofactor at Arg^{306} completely abolishes the ability of the cofactor to interact with factor Xa because of dissociation of the A2 domain of the cofactor, resulting in efficient downregulation of prothrombinase activity (*13*, *15*).

Structural data available to date for factor Va can be summarized as follows: a two-dimensional model (*16*), a theoretical model based on copper binding protein ceruloplasmin that contains 994 residues (Ala^1-Cys^{656} and $Ser^{1546}-Met^{1883}$), part of the A domains (*17*), a homology model for the C1 and C2 domains of factor Va based on the galactose oxidase binding domain (*18*), a crystal structure of the C2 membrane binding domain (*19*), a model of factor Va based on the homology of the cofactor with ceruloplasmin (*20*) proposed by Pellequer et al., and the crystal structure of bovine factor Va_i (a factor Va molecule lacking the entire A2 domain) (*21*).

The model described by Pellequer et al. (*20*) lacks 46 amino acid residues from the carboxyl terminus of the heavy chain (amino acid residues $Ser^{664}-Arg^{709}$). Furthermore, the model does not account for the presence of the solvent. This model will be referred in the text as the "original homology model" since it is used in part as a foundation to propose a completed model for the cofactor. Binding sites for factor Xa and prothrombin have been recently identified on the heavy chain of factor Va (*10*−*12*, *22*−*25*). On the basis of site-directed glycosylation studies, several amino acid residues throughout the entire factor Va molecule were suggested to be interaction sites with factor Xa (*23*). The factor Xa binding site (amino acid residues $Glu^{323}-Val^{331}$) on factor Va (*22*, *26*, *27*) was found to be buried in the original homology model under residues $Tyr^{371}-His^{379}$ of the heavy chain. The prothrombin binding site (amino acid residues $Asp^{695}-Gln^{699}$) (*24*) could not be analyzed since it was located on the carboxyl-terminal region of the heavy chain of factor Va which was missing from the original model. This missing region contains important moieties required for the normal physiological activity of factor Va such as a cleavage site for APC (Arg^{679}) (*15*) and the interactive site for prothrombin (*24*, *25*).

The present study was undertaken to provide a complete model of factor Va that can be used for the investigation and understanding of its physiological functions. After the remodeling of the C1 and C2 domains of factor V and inserting the folded 46 amino acid sequence, the protein was allowed to adjust to the new structural environment by performing molecular dynamics (MD) simulations. We focused our investigation on the factor Xa binding site on the factor Va heavy chain, amino acid residues Glu^{323} and Val^{331} (*12*, *22*), and the recently reported prothrombin binding site on the carboxyl-terminal portion of the heavy chain of the cofactor (*24*, *25*). We have also used our model to understand the mechanism for APC inactivation of the cofactor.

[1] Abbreviations: MD, molecular dynamics; EMBOSS, The European Molecular Biology Open Software Suite; PR-MD, position restraint molecular dynamics; SASA, solvent-accessible surface area; RMSD, root mean square displacement; APC, activated protein C; GROMACS, Groningen machine for chemical simulations; NPT, system with constant number of atoms, pressure, and temperature; TIP4P, transferable intermolecular potential with four points water model; OPLS-AA, optimized potentials for liquid simulations−all atoms force field; factor $Va^{3/5/6}$, factor Va cleaved at Arg^{306}, Arg^{506}, and Arg^{679}; factor $Va^{5/6}$, factor Va cleaved at Arg^{506} and Arg^{679}; factor $Va^{3/6}$, factor Va cleaved at Arg^{306} and Arg^{679}; DSSP, database of secondary structure in proteins; Cα, carbon alpha of an amino acid residue.

METHODS

The recently reported X-ray structure of bovine factor Va_i (*21*) describes a cofactor with a rather different arrangement of the C1 and C2 domains compared with the earlier models (*16*−*20*). In the X-ray structure of bovine factor Va_i, the C1 and C2 domains have their axes of the β barrels in parallel orientation, whereas in the earlier models the axes of the β barrels have a nearly coaxial orientation. In the first step we remodeled the C1 and C2 domains in the original homology model by replacing them with the C1 and C2 domains found in the bovine factor Va_i crystal structure. Sequence alignment performed with The European Molecular Biology Open Software Suite (EMBOSS) server (*28*) showed that there is an 85.5% identity and a 93.1% similarity between the sequence of the C1 and C2 domains of human and bovine factor V. Only 46 amino acids were found to be different between the two species within the C1 and C2 domains. There are no gaps between the two sequences in this region. Therefore, in the first step we changed 46 amino acids from the bovine factor V C1 and C2 sequence into the corresponding amino acids in the human factor V C1 and C2 sequence. The second step in our study was to extend the model of human coagulation factor Va proposed by Pellequer et al. (derived from human ceruloplasmin) (*20*) by adding the missing 46 amino acids at the carboxyl-terminal end of the heavy chain ($Ser^{664}-Arg^{709}$) and perform MD simulations on the completed model. Since we could not find a homologous peptide for the carboxyl-terminal 46 amino acid sequence (based on its primary structure), we used computer simulation techniques to obtain a folded three-dimensional model for this sequence (*29*).

(a) Modeling the Human Factor V C1 and C2 Domains Using the Bovine Factor Va_i *Three-Dimensional Structure as a Template*. The bovine and human primary structures of the C1 and C2 domains were first aligned using the "matcher" program (*30*, *31*) provided by the EMBOSS online server (*28*). Deep View Swiss-PdbViewer (*32*) was then used to change the amino acids from the bovine sequence that were not identical with the human factor V C1 and C2 domain sequence. Forty-six amino acids from the C1 and C2 domains were manually changed using the "mutate" tool from Deep View Swiss-PdbViewer (*32*). The best rotamer for each amino acid, which is the form of the amino acid with the lowest score, was chosen each time (see Table 1 in Supporting Information). The modeled C1 and C2 domains were then inserted in the original homology model by fitting the Cα atoms of two amino acid groups. The first group is formed by amino acids Arg^{1877}, Asp^{1878}, and Cys^{1879} and is part of the original homology model, whereas Arg^{1864}, Glu^{1865}, and Cys^{1866} make a second group, which is part of the bovine factor Va_i structure. These groups were fitted with the "fit" tool from Deep View Swiss-PdbViewer. The ϕ and ψ angles of Cys^{1879} were changed according to the values found in the bovine factor Va_i crystal structure. The steric strain on Glu^{1608} (due to the insertion of C1 and C2 domains)

was removed by using a new rotamer generated by Deep View Swiss-PdbViewer, which has the lowest score (−2) of a set of eight generated rotamers.

(b) Modeling the Calcium and Copper Binding Sites on Factor Va. The original homology model contains two Ca^{2+} ions and one Cu^{2+} ion. The crystal structure of bovine factor Va_i (*21*) shows the Cu^{2+} ion in the vicinity of amino acid residues His^{1802}, His^{1804}, and Asp^{1844}. We have included in our model one Cu^{2+} and two Ca^{2+} according to the literature (*21*, *33*, *34*). Residues Asp^{111} and Asp^{112} together with the oxygen from the carbonyl group of Lys^{93} and Glu^{108} were identified to coordinate a Ca^{2+} ion on factor Va in the crystal structure of bovine factor Va_i. These data confirm the existence of the earlier described Ca^{2+} binding site in the region $Glu^{96}-Asp^{111}$ of the cofactor (*33*). Previous findings have also described two Ca^{2+} binding sites with lower affinity (*34*). Therefore, one of the Ca^{2+} ions that was not found in the bovine factor Va_i crystal structure but was modeled in the original homology model, i.e., in the vicinity of amino acid residues Asp^{1579}, Glu^{1576}, Glu^{1572}, and Glu^{1583}, was retained in the present study. The other Ca^{2+} ion was placed in the proximity of Asp^{111}, Asp^{112}, Lys^{93}, and Glu^{108} whereas the Cu^{2+} ion was positioned nearby His^{1802}, His^{1804}, and Asp^{1844}. Distances from the ions to the corresponding amino acids were adjusted on the basis of the bovine factor Va_i crystal structure geometry.

(c) Preparation of the MD Simulations. The modeling of the complete factor Va structure required several MD simulations [performed with the GROMACS (*35*−*37*) program]. For all systems subjected to simulations we used the same parameters. These systems are (i) high-temperature-driven simulation of the incomplete factor Va model, (ii) folding of the 46 amino acid peptide, and (iii) relaxation of the new model. The number of particles, the groups chosen for temperature and pressure coupling, the simulation time, and temperature were chosen according to the needs of each simulation. Parameters that differ from one simulation to another are described in the following sections.

For the MD simulations the protein was placed in a water box by setting the distance between the box walls and protein/peptide to 5 Å. Initial velocities for atoms were taken from the Maxwellian distribution at 300 K. For solvent we used the transferable intermolecular potential with four points water model (TIP4P) (*38*). An OPLS-AA parameter set was used to describe the interactions for all atoms of the system (*39*). Ions (Cl^- or Na^+) were added when the system was positively or negatively charged to keep the system neutral. Ions were added using the program "genion" [a GROMACS (*35*−*37*) tool] by replacing water molecules with the corresponding ions. The positioning of the ions was performed by using an electrostatic potential criterion with a 0.9 Å Coulomb cutoff and setting the minimum distance between ions to 6 Å. The LINCS algorithm was used for bond constraints (*40*).

Energy minimizations were carried out with the steepest-descent method with the initial step set to 0.1 Å. The neighbor list updated frequency was set to 10, and we used the "grid" option for neighbor search. Periodic boundary conditions were employed in all three dimensions. The cutoff distance for the short-range neighbor list was set to 9 Å. Long-range electrostatic interactions were treated using the particle mesh Ewald summation method (*41*, *42*). Ewald summation was performed in all three dimensions. The fast Fourier transform grid dimension was set to 1.6 Å, and the interpolation order was set to 4. During energy minimization bonds were not constrained.

Position restraint molecular dynamics simulation (PR-MD) was performed using the "md" integrator with all bonds constrained and all heavy atoms from the protein restrained to move around their initial position with a harmonic oscillator function. The integration step was set to 2 fs, and the total PR-MD simulation was 20 ps long. Long-range electrostatic interactions were calculated as in the energy minimization step. The system was treated as an NPT ensemble (constant number of atoms, constant pressure, and constant temperature). The reference temperature was set to 300 K for those simulations that did not employ a high-temperature-driven conformational search. The simulation was carried out at constant pressure using Parrinello−Rahman (*43*) isotropic pressure coupling with the compressibility set to 4.5×10^{-5} bar^{-1} and a reference pressure of 1 bar. Parameters used in the molecular dynamics simulation were the same as described at the PR-MD step, except that the heavy atoms (all atoms except the hydrogen atoms) were allowed to move freely.

(d) High-Temperature-Driven Conformational Search for the Incomplete Factor Va Model with the Newly Modeled C1 and C2 Domains. The factor Va model that contained the newly modeled C1 and C2 domains but without the 46 amino acids from the carboxyl terminus, i.e., $Asp^{663}-Arg^{709}$, was subjected to 100 ps of high-temperature-driven MD simulation. The purpose of this short simulation was to relax the region $Val^{654}-Asp^{663}$ before adding the 46 amino acid peptide. The region $Val^{654}-Asp^{663}$ is a straight coil having one kink due to Pro^{658}. All other parameters were chosen to be the same as described above in the Preparation of the MD Simulations section except for the temperature that was set to 400 K. Because the total charge of the system was +1, one Cl^- ion was added to the system before starting the simulation by replacing one water molecule. For the Ca^{2+} and Cu^{2+} ions we used the parameters as described by Åqvist et al. (*44*) (mass = 40.08000 amu, charge = 2.000 eu, σ = 0.241203 nm, ϵ = 1.88136 kJ/mol) and Reichert et al. (*45*) (mass = 63.546 amu, charge = 2.000 eu, σ = 0.208470 nm, ϵ = 4.76976 kJ/mol), respectively. The system was coupled to a Berendsen thermostat (*46*) with a reference temperature of 400 K. The final snapshot from the 100 ps simulation was used to insert the folded 46 amino acid peptide into the factor Va molecule.

(e) Folding of the 46 Amino Acid Peptide. The last residue, Asp^{663}, from the heavy chain of the original homology model of factor Va (*20*) protrudes outward from the protein surface (e.g., Asp^{663} is 20.4 Å away from the closest solvent accessible residue, Val^{654}, which is part of an outer loop). We thus decided to fold the peptide in a separate simulation before attaching it to factor Va. The starting model of the peptide had three straight-line backbone domains separated by two kinks. The final three-dimensional model of the peptide was obtained following three simulations: (i) 14 ns simulation at 300 K, (ii) 1 ns high-temperature conformational search simulation at 400 K, and (iii) 2 ns simulation at 300 K for equilibration. All other simulation parameters used are described in the Preparation of the MD Simulations section. Because the total charge of the system was −7, seven

water molecules were replaced with seven Na^+ ions. The system was coupled to the Berendsen thermostat (*46*) using a reference temperature of 300 K for the first and third simulation and 400 K for the high-temperature conformational search. The root mean square displacement (RMSD) of the Cα atoms was plotted for the final simulation to ascertain equilibration of the system. The starting coil model of the peptide [based on its primary structure (*8*)] was built using the Pymol program (*47*). After a 1 ns simulation (temperature-driven conformational search) in water we performed a 2 ns simulation to equilibrate the system. The final snapshot was saved and after minimization was inserted in the incomplete factor Va model.

(f) Insertion of the Folded Peptide into the Human Factor Va Model. The minimized three-dimensional model of the peptide was inserted in the original homology model containing the newly modeled C1 and C2 domains. Extending the factor Va heavy chain required two steps: (1) making the peptide bond between Asp^{663} and Ser^{664} (Ser^1 in the folded peptide) and (2) performing MD simulation of the extended factor Va molecule in solution. The peptide bond, connecting the carboxyl-terminal residue of the incomplete model, Asp^{663}, with the amino-terminal residue of the folded peptide (Ser^{664} in factor Va), was made with the Deep View Swiss-PdbViewer program (*32*). The ϕ and ψ angles of residue Asp^{663} were adjusted in such a manner that the ϕ and ψ angles of the inserted 46 amino acid residues are positioned in the allowed regions of the Ramachandran plot (*48*). To ascertain peptide equilibration, the RMSD of Cα of the peptide was plotted as a function of time. The hydrogen bond network formed following peptide folding was also verified (see Table 2 in Supporting Information). The final simulation removes the steric strain and allows the peptide to adjust to the factor Va three-dimensional model.

(g) MD Simulation of the Completed Factor Va Model. The new model of the complete factor Va molecule was solvated in water and subjected to a 1.4 ns MD simulation in order to allow the newly inserted peptide and the newly modeled C1 and C2 domains to adjust to the model of factor Va and maximize their interaction with the neighboring residues of the cofactor. Parameters used are described in the Preparation of the MD Simulations section.

(h) MD Simulation of the APC-Cleaved Factor Va. The factor Va model obtained following 1.4 ns simulation was used to test the behavior of the factor Va-derived fragments following APC cleavage (*13*, *15*). We prepared a cleaved factor Va molecule at Arg^{306}, Arg^{506}, and Arg^{679}, a molecule that mimics APC-induced inactivation of the cofactor on the membrane surface (factor $Va^{3/5/6}$). We have also studied factor Va cleaved at Arg^{506} and Arg^{679}, a molecule that mimics APC cleavage of the cofactor in the absence of a membrane surface (factor $Va^{5/6}$), and factor Va cleaved at Arg^{306} and Arg^{679}, a molecule that mimics APC cleavage of membrane-bound factor Va^{LEIDEN} (factor $Va^{3/6}$). Simulation parameters were the same as previously described for the intact model of factor Va. All simulations were performed for 2 ns. Distances between the mass centers of the generated fragments following cleavage of the heavy chain and the light chain were calculated using the "g_dist" utility program from GROMACS.

RESULTS AND DISCUSSION

Verification of the Model. (a) Superposition of the New Model with the Model Obtained from the Bovine Factor Va_i Crystal Structure. Following 1.4 ns simulation, the equilibration of the system was verified by plotting the change in temperature, potential energy, and RMSD of Cα of the factor Va molecule versus time (see Figure 1 in Supporting Information). Further analysis of the trajectory of the complete factor Va model was made using the equilibrated portion of the simulation (i.e., from 0.8 to 1.4 ns). The DSSP (*49*) program was used to assign the secondary structure.

The recently solved crystal structure of bovine factor Va_i provides a structure for a significant part of the A1, A3, C1, and C2 domains of the bovine cofactor (*21*). However, the crystal structure lacks the entire A2 domain and several segments throughout the entire molecule. In contrast, we are providing a three-dimensional model encompassing the entire structure of the factor Va molecule. To validate the amino acid sequences of the segments of our model, not present in the bovine factor Va_i structure (i.e., several segments throughout the A1 and A3 domains and the entire A2 domain), we superimposed all homologous regions present in both the crystal structure and our model (see Figure 2 in Supporting Information). Seven out of nine RMSD values were found to be in the range 1.6−2.5 Å. The other two regions corresponding to a total number of 88 and 422 amino acid residues have an RMSD of 4.77 and 4.64 Å, respectively (Figure 2g,i in Supporting Information). The large RMSD observed between the crystal structure of bovine factor Va_i and the model of human factor Va presented herein within regions Asn^{1670}−Glu^{1757} and Lys^{1773}−Tyr^{2196} can be explained by the fact that in the crystal structure of bovine factor Va_i the amino and carboxyl termini of the segments move freely, while the corresponding amino acids in the model of human factor Va are engaged in peptide bonds and follow a structure dictated by all other amino acids in the group (Figure 2g,i in Supporting Information). It is noteworthy that while the alignment of residues Asn^{1760}−Met^{2182} (from bovine factor Va_i) with the corresponding region from the model of human factor Va (Lys^{1773}−Tyr^{2196}) results in a large RMSD, the alignments of two large segments within these regions, representing the entire C1 and C2 domains as well as residues Lys^{1773}−Gly^{2032} taken separately, have RMSD values of 1.79 and 1.56 Å, respectively. In conclusion, the comparison between the model of human factor Va and the crystal structure of bovine factor Va_i provides a valuable confirmation for our model.

Verification of the Model. (b) Superposition of the New Model with the Model Obtained from the Crystal Structure of Ceruloplasmin. Polypeptide segments available from the ceruloplasmin crystal structure (PDB code 1KCW) (*50*) were also superimposed with the corresponding fragments from the model of factor Va. RMSD values between the model and four fragments from ceruloplasmin, i.e., Lys^1−Cys^{338}, Ile^{347}−Pro^{474}, Val^{483}−Pro^{884}, and Arg^{892}−Asn^{1040}, were found to be 1.58, 1.32, 1.72, and 1.83 Å, respectively (not shown). These data together with the data presented above validate our model and provide for the first time a working model of a complete human factor Va molecule in solution. The model has been deposited in the Protein Data Bank, PDB code 1Y61.

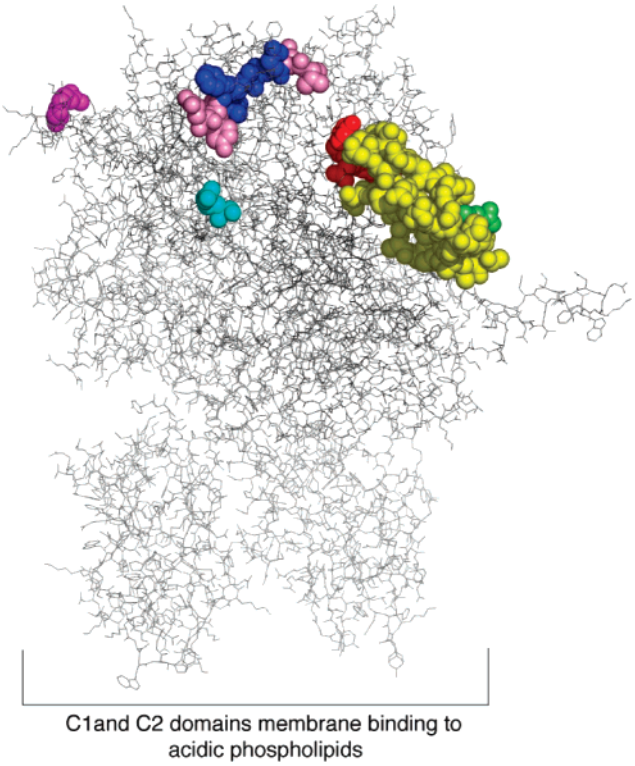

FIGURE 1: A model of the complete human factor Va molecule. The extremities of the factor Xa binding site are shown in pink (residues Glu^{323}, Tyr^{324}, Glu^{330}, and Val^{331}) with the rest shown in blue (residues Phe^{325}−Glu^{329}). Red spheres represent the prothrombin binding site on factor Va (residues Asp^{695}−Gln^{699}). APC cleavage sites Arg^{306}, Arg^{506}, and Arg^{679} are shown in magenta, cyan, and lime, respectively. Yellow spheres show the rest of the 46 newly added amino acids (Ser^{664}−Arg^{679}, Lys^{680}−Ala^{694}, and Asn^{700}−Arg^{709}). The position of the C1 and C2 domains is also depicted to show the relative position of the important moieties of the heavy chain of the cofactor from the membrane surface.

Factor Xa Binding Sites on Factor Va. Figure 1 shows the complete factor Va molecule following 1.4 ns simulation with the C1 and C2 membrane-binding domains together with a portion of the factor Xa binding site of the cofactor located on the A2 domain. Amino acid residues Glu^{323}, Tyr^{324}, Glu^{330}, and Val^{331} (*22*, *26*) (shown in pink) represent the extremities of the factor Xa binding site on factor Va (*22*), whereas amino acid residues Asp^{695}−Gln^{699} (in red) illustrate a prothrombin interactive site on the cofactor (*24*). Amino acid residues Tyr^{371}−His^{379} (in gray) correspond to amino acids that cover the factor Xa binding site. Amino acid residues Ser^{664}−Ala^{694} and Asn^{700}−Arg^{709} (in yellow) represent the rest of the newly added 46 amino acid residue carboxyl-terminal peptide.

We next studied the change in the conformation of amino acid residues Tyr^{371}−His^{379}, which partially cover the factor Xa binding site on factor Va, following the simulation. The RMSD of these amino acids was calculated with respect to amino acid residues Met^{410} and Lys^{408}. Similar measurements were performed with the amino acid stretch Glu^{323}−Val^{331}. We found that the displacement (with respect to Lys^{308}) of amino acid residues Glu^{372}−Lys^{378} was twice the displacement of amino acid residues Glu^{323}−Val^{331}. Tyr^{371} was found to participate in a hydrogen bond [Tyr^{371} donor atom^{OH}−hydrogen atom ^{HH}−acceptor Glu^{329} atom^{OE2} using atom nomenclature as described (*51*)] that lasts 800 ps out of 1.4 ns simulation, which is statistically considered a persistent hydrogen bond (*52*). Lys^{378} has two hydrogen bonds before simulation with Glu^{372}, but only one hydrogen bond is preserved during simulation. It appears that the existence of these hydrogen bonds is at the origin of the small RMSD observed for amino acid residues Tyr^{371} and His^{379} during the 1.4 ns simulation. On the other hand, amino acid sequence Glu^{372}−Lys^{378} is part of a loop and is not involved in hydrogen bonding (which would restrict its movement with respect to amino acid residues Glu^{323}−Val^{331}).

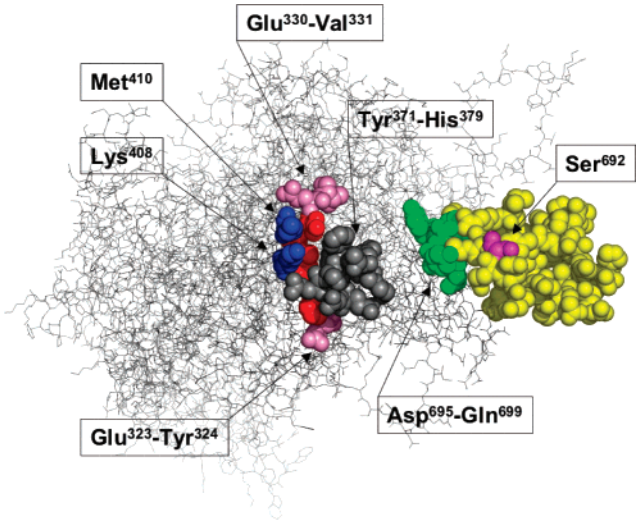

FIGURE 2: Structural details of factor Xa and the prothrombin interactive site on factor Va. Gray spheres (residues Tyr^{371}−His^{379}) represent residues that block solvent accessibility of the factor Xa binding site; pink spheres (Glu^{330}−Val^{331} and Glu^{323}−Tyr^{324}) and red spheres (Phe^{325}−Glu^{329}) show portions from factor Xa binding site. The prothrombin binding site on factor Va (amino acid residues Asp^{695}−Gln^{699}) is shown in green while amino acid residue Ser^{692} is shown in violet. Amino acid residues Met^{410} and Lys^{408} are shown in blue; the rest of the newly added 46 amino acid peptide (Ser^{664}−Glu^{691}, Asp^{693}−Ala^{694}, and Asn^{700}−Arg^{709}) is shown in yellow.

It has been hypothesized (*22*) that, due to physiological needs, amino acid residues Tyr^{371}−His^{379} could hinder the solvent accessibility of Tyr^{324}−Phe^{325}, which are involved in binding factor Xa (i.e., Glu^{323}−Val^{331}). Perhaps factor Va exposes residues Tyr^{324}−Phe^{325} only when bound to a procoagulant cell surface. This assumption (*22*) has been made on the basis of studies of the incomplete homology model. Further, the amino acid sequence missing in the original model (Ser^{664}−Arg^{709}) is relatively close in space to the sequence Glu^{323}−Val^{331} (22.42 Å between Cα atoms of Tyr^{698} and Val^{331}). After 1.4 ns simulation, the interaction of the newly added amino acid residues with amino acid segment Tyr^{371}−His^{379} led to an increased exposure of amino acids Tyr^{324} and Phe^{325} (see Supporting Information, Figure 3B); however, despite this significant change during simulation amino acid residues Tyr^{324} and Phe^{325} are still not solvent accessible [the solvent-accessible surface area (SASA) does not increase after simulation]. Figure 2 shows details of the factor Xa binding site on factor Va after 1.4 ns simulation. Even though amino acid residues Tyr^{371}−His^{379} (Figure 2, gray) are shifted by 8.0 Å after simulation, Met^{410} and Lys^{408} (Figure 2, dark blue) are still partially blocking access to amino acid segment Glu^{323}−Val^{331}.

As recently demonstrated, amino acids Glu^{323}, Tyr^{324}, Glu^{330}, and Val^{331} are essential in binding factor Xa to factor Va (*26*). It has been shown experimentally (*26*) that amino

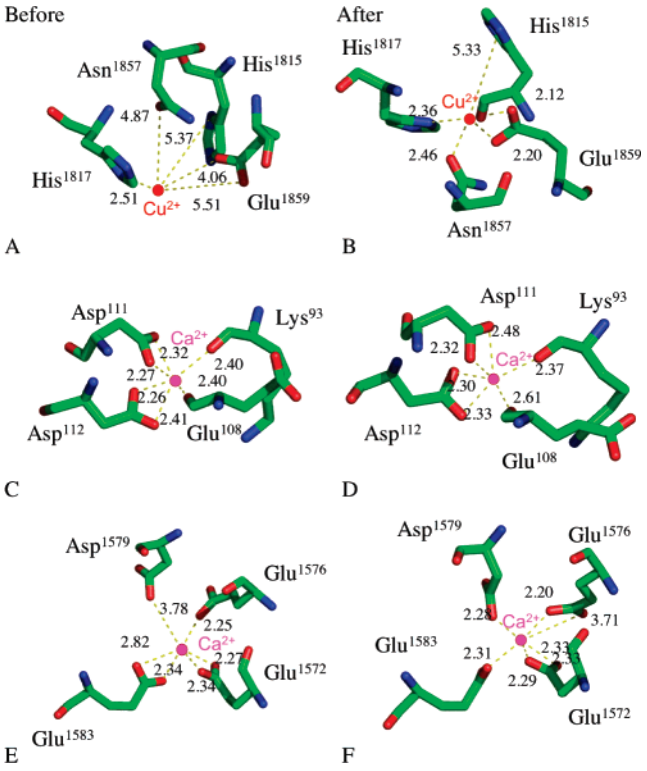

FIGURE 3: Cu^{2+} and Ca^{2+} ion detail before and after 1.4 ns simulation. Amino acid residues involved in binding of the Cu^{2+} and Ca^{2+} ions are shown with sticks. Panels A and B show the Cu^{2+} ion coordination before and after the simulation, respectively. Panels C, D and E, F show the two Ca^{2+} ions before and after simulations. Distances, in angstroms, are shown from the Cu^{2+} and Ca^{2+} ions to the nearest amino acid residues.

acid residues Glu^{330} and Val^{331} are more important for binding of factor Xa than amino acid residues Glu^{323} and Tyr^{324}. Since amino acids Glu^{330} and Val^{331} are exposed to the solvent, they could be responsible for the weak interaction observed between factor Va and factor Xa in solution [i.e., the binding site of factor Xa on factor Va is not entirely solvent accessible when the proteins are not bound to a procoagulant cell membrane surface (*53*)].

Amino acid residues Glu^{467}, Ala^{511}, Arg^{652}, and His^{1683}, previously shown to represent a surface for factor Xa binding, remained solvent exposed after simulations (*23*). However, it was found that SASA of Glu^{467} slightly decreased during simulations, mainly due to the new hydrogen bond formation with Lys^{607}. During simulations, Arg^{652} formed hydrogen bonds with Thr^{571} and Asp^{653}, while His^{1683} formed hydrogen bonds with Glu^{1560}.

Calcium and Copper Binding Sites on Factor Va. Ion binding sites are shown in Figure 3 together with the distances prior to and after simulation. Before simulation, the distance from the carboxy oxygens of Glu^{1859} to the Cu^{2+} ion was found to be in the range of 4−5.5 Å (Figure 3A). Following simulation, the same distance decreased to ∼2.12−2.20 Å (Figure 3B). The modeled Cu^{2+} ion, using factor Va_i as a template, is not at the interface of A1 and A3 as previously suggested (*20*); hence it may not be directly involved in the association of the heavy and light chains. As proposed (*21*), the Cu^{2+} ion may have a role in providing additional stabilization of the heavy and light chains. The closest amino acid residue from the heavy chain is found at a distance of 5 Å from the Cu^{2+} ion (Gln^{87}). This model assumes that the heavy and light chains are held together primarily by means of hydrogen bonds between the A1 and A3 domains as suggested (*21*). The distances between one Ca^{2+} ion to the neighboring residues show no significant changes (see Figure 3C before simulations and Figure 3D after simulations). Amino acids Asp^{1579} and Glu^{1583} are found to be slightly closer to the other Ca^{2+} ion after simulation (2.28 and 2.31 Å, respectively, Figure 3F) when compared with the same arrangement before simulation (3.78 and 2.82 Å, respectively, Figure 3E).

Prothrombin Binding Site on Factor Va. In the newly extended factor Va model, the prothrombin binding site [residues Asp^{695}−Gln^{699} (*24*)] is in the proximity of factor Xa binding sites, that is, ∼22 Å to residues Glu^{323}−Val^{331} (*22*) and ∼12−36 Å to residues Glu^{467}, Ala^{511}, Arg^{652}, and His^{1683} (*23*). The RMSD from the initial model calculated for all five residues, Asp^{695}−Gln^{699}, shows that Asp^{695} and Tyr^{696} have the largest RMSD value (8 and 6 Å, respectively), while Asp^{697}, Tyr^{698}, and Gln^{699} have smaller, but similar values compared to each other (∼2 Å). After simulations, the phenyl moieties of amino acid residues Tyr^{696} and Tyr^{698} are facing toward the outside the protein, whereas Gln^{699}, even though it is solvent accessible, is found in a pocket close to Arg^{709}.

Dissociation of the A2 Domain from APC-Cleaved Factor Va. All three cleavage sites of APC on the factor Va model are solvent accessible (see Figure 1, Arg^{306} in magenta, Arg^{506} in cyan, and Arg^{679} in lime). Previous data using bovine factor Va and immunoprecipation techniques have suggested that factor Va inactivation is a consequence of both cleavage and dissociation of the A2 domain from the rest of the molecule (*13*). However, the latter data were unable to distinguish which of the two events was the major contributing factor to the inactivation process. Similar biochemical data are not available for the human molecule. Moreover, using an interdomain engineered disulfide bond recombinant factor Va molecule, it was suggested that cleavage at Arg^{506} and Arg^{306} is critical for inactivation (*54*). This latter study used a recombinant human factor Va molecule with a disulfide bond between Cys^{609} and Cys^{1691}. Finally, it has been shown that inactivation of factor V^{LEIDEN} is much slower than inactivation of normal plasma factor Va (*55*−*58*). However, one question remains unanswered: Is factor Va^{LEIDEN} inactivation slower because of the slower rate of cleavage at Arg^{306} (because of the absence of cleavage at Arg^{506}) or because of the slower rate of dissociation of the A2 domain from the rest of the molecule?

To ascertain the role of cleavages at Arg^{306} and Arg^{506} by APC for human factor Va inactivation, a 2 ns simulation of factor Va fragments derived from membrane-dependent inactivation of factor Va by APC was performed using the factor Va model developed herein (factor $Va^{3/5/6}$, Figure 4A). The data reveal that the two A2 domain-derived fragments (Asn^{307}−Arg^{506} and Gly^{507}−Arg^{679}) have persistently larger RMSD values than the A1 domain (amino acid residues Ala^{1}−Arg^{306}, Figure 4A). The number of hydrogen bonds between the A2 domain-derived fragments and the light chain was also found to decrease. Distance analyses, between the A2 domain-derived fragments and a contact region from the light chain, residues Val^{1736}−Leu^{1836}, show that the distance between fragments composed of amino acids Asn^{307}−Arg^{506} and Gly^{507}−Arg^{679} increases by 1.8 and 2.2 Å, respectively,

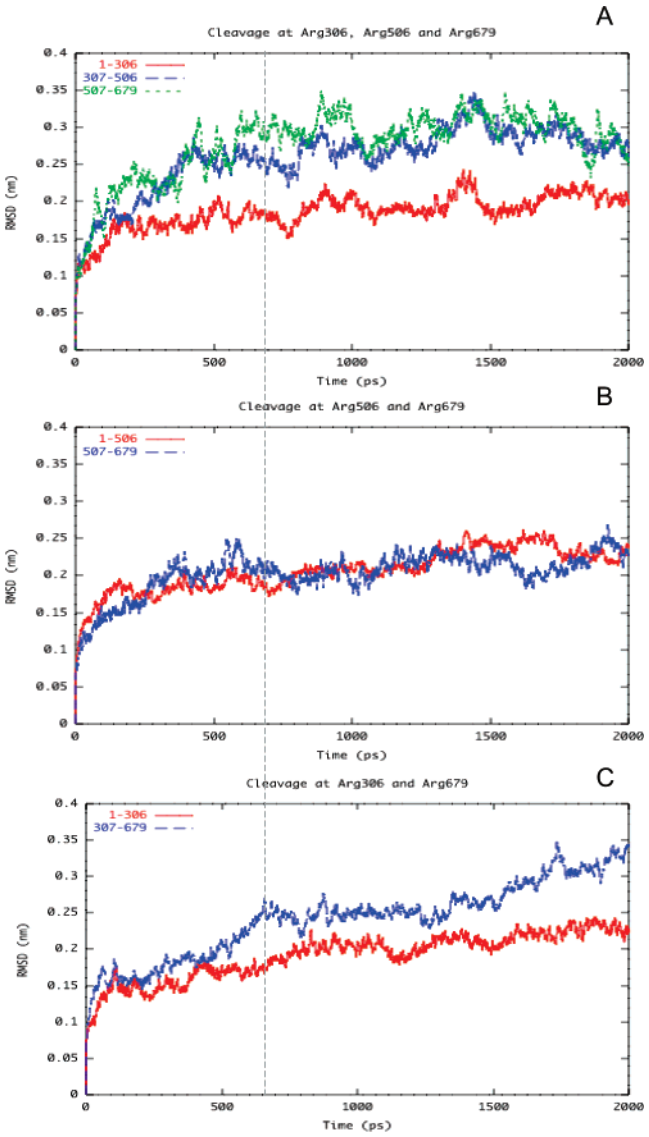

FIGURE 4: APC-induced factor Va inactivation. Panel A shows the factor $Va^{3/5/6}$ RMSD (nm) versus simulation time (ps) of fragments $Ala^{1}-Arg^{306}$ (red line), $Asn^{307}-Arg^{506}$ (blue line), and $Gly^{507}-Arg^{679}$ (green line). Panel B shows the factor $Va^{5/6}$ RMSD of fragments $Ala^{1}-Arg^{506}$ (red line) and $Gly^{507}-Arg^{679}$ (blue line). Panel C shows the factor $Va^{3/6}$ (factor Va^{LEIDEN}) RMSD of fragments $Ala^{1}-Arg^{306}$ (red line) and $Asn^{307}-Arg^{679}$ (blue line).

following 300 ps and remains constant following a 2 ns simulation (Figure 4A, blue and green). In contrast, the distance of the A1 domain of factor Va ($Ala^{1} - Arg^{306}$) from the same contact point of the light chain remains approximately the same following a 2 ns simulation (Figure 4A, red). Thus, it appears that while the A1 domain remains connected to the light chain by noncovalent interaction, the distance between A2 domain fragments and the rest of the molecule increases. These data strongly suggest that the A2 domain of the cofactor dissociates from the rest of the molecule following APC cleavage.

The simulations of factor $Va^{5/6}$ (simulation of factor Va cleaved by APC in the absence of a membrane surface at Arg^{506} and Arg^{679}) show that the two resulting fragments, i.e., $Ala^{1}-Arg^{506}$ and $Gly^{507}-Arg^{679}$, have the same RMSD values (Figure 4B, red and blue). Distance analysis of these two fragments shows that the distance between these segments and residues $Val^{1736}-Leu^{1836}$ of the light chain does not increase significantly during the 2 ns simulation. Additionally, the hydrogen-bonding network between these fragments and the light chain is also preserved. Finally, a similar analysis of factor $Va^{3/6}$ (simulation of APC-cleaved membrane-bound factor Va^{LEIDEN}, Figure 4C, red and blue) reveals that cleavage at Arg^{306} even in the absence of cleavage at Arg^{506} results in the release of the A2 domain of the cofactor in a time frame similar to that observed for plasma factor $Va^{3/5/6}$ (650 ps). These data are original and provide compelling evidence suggesting that inactivation of factor Va occurs because of dissociation of the A2 domain of factor Va and loss of a portion of the factor Xa binding domain.

Overall, the data imply that cleavage of the cofactor at Arg^{506} is not required for bisection of the A2 domain in two fragments. Cleavage of factor Va at Arg^{506} is rather required to facilitate cleavage at Arg^{306} as suggested (*55*). Thus, slower inactivation of factor Va^{LEIDEN} by APC occurs because of delayed cleavage at Arg^{306}, which in turn is required for dissociation of the A2 domain from the rest of the molecule. Altogether, these data demonstrate that factor Va inactivation occurs in a similar manner as factor VIIIa inactivation following dissociation of the enzyme binding site from the rest of the cofactor molecule (*59*−*61*). However, while inactivation of the latter occurs spontaneously at pH 7.4, factor Va inactivation is induced following cleavage by APC at Arg^{306} (*15*).

CONCLUSIONS

We are presenting in this work for the first time a complete structure of coagulation factor Va and have studied the dynamics of the several amino acid domains in solution by molecular dynamics simulations. Our analysis of the molecular dynamics simulation data of solvated human factor Va suggests that amino acids Met^{410} and Lys^{408}, together with amino acid residues $Tyr^{371}-His^{379}$, are partially masking the binding site of factor Va for factor Xa in solution (amino acid residues 323−331). However, amino acids Glu^{323}, Tyr^{324}, Glu^{330}, and Val^{331} representing the extremities of the factor Va binding site for factor Xa are exposed. These data suggest that factor Xa most likely interacts with these latter amino acids in solution, resulting in a bimolecular interaction characterized by low affinity (0.8 μM). Upon binding of the proteins to a procoagulant surface exposed upon injury of the endothelium, the rest of the factor Xa binding site on factor Va is exposed, resulting in a high-affinity bimolecular interaction (more points of contact between the two proteins). Exposure of the entire binding site should result in a strong interaction between factors Va and Xa, which is necessary for efficient functioning of the prothrombinase complex in vivo (*3*, *22*). Altogether, the data suggest that amino acid residues $Tyr^{371}-His^{379}$ play the role of a control switch, modulating the ability of factor Va to interact with factor Xa.

The completed model of factor Va provides evidence that inactivation of the cofactor by APC is due to dissociation of the A2 domain and that delayed inactivation of factor Va^{LEIDEN} as compared to plasma factor Va is due to the slower rate of cleavage at Arg^{306} as suggested (*55*).

SUPPORTING INFORMATION AVAILABLE

Two tables and three figures are provided. Rotamers and the best scores for the changed amino acids in the bovine C1 and C2 domains are presented in Table 1. The hydrogen-bonding network found in the folded 46 amino acid peptide is described in Table 2. Equilibration of the factor Va molecule is shown in Figure 1. Figure 2 shows the superposed segments from the new factor Va model obtained after 1.4 ns MD simulation with corresponding fragments from the crystal structure of bovine factor Vai. The factor Xa binding side on factor Va is shown in Figure 3. This material is available free of charge via the Internet at http://pubs.acs.org.

REFERENCES

1. Mann, K. G., and Kalafatis, M. (2003) Factor V: a combination of Dr Jekyll and Mr Hyde, *Blood 101*, 20−30.
2. Kalafatis, M., Egan, J. O., van't Veer, C., Cawthern, K. M., and Mann, K. G. (1997) The regulation of clotting factors, *Crit. Rev. Eukaryotic Gene Expression 7*, 241−280.
3. Nesheim, M. E., Taswell, J. B., and Mann, K. G. (1979) The contribution of bovine factor V and factor Va to the activity of prothrombinase, *J. Biol. Chem. 254*, 10952−10962.
4. Davie, E. W., Fujikawa, K., and Kisiel, W. (1991) The coagulation cascade: initiation, maintenance, and regulation, *Biochemistry 30*, 10363−10370.
5. Krishnaswamy, S., Jones, K. C., and Mann, K. G. (1988) Prothrombinase complex assembly. Kinetic mechanism of enzyme assembly on phospholipid vesicles, *J. Biol. Chem. 263*, 3823−3834.
6. Krishnaswamy, S. (1990) Prothrombinase complex assembly. Contributions of protein-protein and protein-membrane interactions toward complex formation, *J. Biol. Chem. 265*, 3708−3718.
7. Boskovic, D. S., Bajzar, L. S., and Nesheim, M. E. (2001) Channeling during prothrombin activation, *J. Biol. Chem. 276*, 28686−28693.
8. Jenny, R. J., Pittman, D. D., Toole, J. J., Kriz, R. W., Aldape, R. A., Hewick, R. M., Kaufman, R. J., and Mann, K. G. (1987) Complete cDNA and derived amino acid sequence of human factor V, *Proc. Natl. Acad. Sci. U.S.A. 84*, 4846−4850.
9. Tucker, M. M., Foster, W. B., Katzmann, J. A., and Mann, K. G. (1983) A monoclonal antibody which inhibits the factor Va: factor Xa interaction, *J. Biol. Chem. 258*, 1210−1214.
10. Guinto, E. R., and Esmon, C. T. (1984) Loss of prothrombin and of factor Xa-factor Va interactions upon inactivation of factor Va by Activated Protein C, *J. Biol. Chem. 259*, 13986−13992.
11. Annamalai, A. E., Rao, A. K., Chiu, H. C., Wang, D., Duttâ-Roy, A. K., Walsh, P. N., and Colman, R. W. (1987) Epitope mapping of functional domains of human factor Va with human and murine monoclonal antibodies. Evidence for the interaction of heavy chain with factor Xa and calcium, *Blood 70*, 139−146.
12. Kalafatis, M., Xue, J., Lawler, C. M., and Mann, K. G. (1994) Contribution of the heavy and light chains of factor Va to the interaction with factor Xa, *Biochemistry 33*, 6538−6545.
13. Mann, K. G., Hockin, M. F., Begin, K. J., and Kalafatis, M. (1997) Activated protein C cleavage of factor Va leads to dissociation of the A2 domain, *J. Biol. Chem. 272*, 20678−20683.
14. Rosing, J., Hoekema, L., Nicolaes, G. A., Thomassen, M. L. G. D., Hemker, H. C., Varadi, K., Schwartz, H. P., and Tans, G. (1995) Effects of protein S and factor Xa on peptide bond cleavages during inactivation of factor Va and factor VaR506Q by activated protein C, *J. Biol. Chem. 270*, 27852−27858.
15. Kalafatis, M., Rand, M. D., and Mann, K. G. (1994) The mechanism of inactivation of human factor V and human factor Va by activated protein C, *J. Biol. Chem. 269*, 31869−31880.
16. Stoylova, S., Mann, K. G., and Brisson, A. (1994) Structure of membrane-bound human factor Va, *FEBS Lett. 351*, 330−334.
17. Villoutreix, B. O., and Dahlbäck, B. (1998) Structural investigation of the A domains of human blood coagulation factor V by molecular modeling, *Protein Sci. 7*, 1317−1325.
18. Pellequer, J. L., Gale, A. J., Griffin, J. H., and Getzoff, E. D. (1998) Homology models of the C domains of blood coagulation factors V and VIII: a proposed membrane binding mode for FV and FVIII C2 domains, *Blood Cell. Mol. Dis. 24*, 448−461.
19. Macedo-Ribeiro, S., Bode, W., Huber, R., Quinn-Allen, M. A., Kim, S. W., Ortel, T. L., Bourenkov, G. P., Bartunik, H. D., Stubbs, M. T., Kane, W. H., and Fuentes-Prior, P. (1999) Crystal structures of the membrane-binding C2 domain of human coagulation factor V, *Nature 402*, 434−439.
20. Pellequer, J. L., Gale, A. J., Getzoff, E. D., and Griffin, J. H. (2000) Three-dimensional model of coagulation factor Va bound to activated protein C, *Thromb. Haemostasis 84*, 849−857.
21. Adams, T. E., Hockin, M. F., Mann, K. G., and Everse, S. J. (2004) The crystal structure of activated protein C-inactivated bovine factor Va: Implications for cofactor function, *Proc. Natl. Acad. Sci. U.S.A. 101*, 8918−8923.
22. Kalafatis, M., and Beck, D. O. (2002) Identification of a binding site for blood coagulation factor Xa on the heavy chain of factor Va. Amino acid residues 323−331 of factor V represent an interactive site for activated factor X, *Biochemistry 41*, 12715−12728.
23. Steen, M., Villoutreix, B. O., Norstrom, E. A., Yamazaki, T., and Dahlbäck, B. (2002) Defining the factor Xa-binding site on factor Va by site-directed glycosylation, *J. Biol. Chem. 277*, 50022−50029.
24. Beck, D. O., Bukys, M. A., Singh, L. S., Szabo, K. A., and Kalafatis, M. (2004) The contribution of amino acid region ASP695-TYR698 of factor V to procofactor activation and factor Va function, *J. Biol. Chem. 279*, 3084−3095.
25. Kalafatis, M., Beck, D. O., and Mann, K. G. (2003) Structural requirements for expression of factor Va activity, *J. Biol. Chem. 278*, 33550−33561.
26. Singh, L. S., Bukys, M. A., Beck, D. O., and Kalafatis, M. (2003) Amino acids Glu323, Tyr324, Glu330, and Val331 of factor Va heavy chain are essential for expression of cofactor activity, *J. Biol. Chem. 278*, 28335−28345.
27. Bukys, M. A., Blum, M. A., Kim, P. Y., Brufatto, N., Nesheim, M. E., and Kalafatis, M. (2005) Incorporation of factor Va into prothrombinase is required for coordinated cleavage of prothrombin by factor Xa, *J. Biol. Chem. 280*, 27393−27401.
28. Rice, P., Longden, I., and Bleasby, A. (2000) EMBOSS: The European Molecular Biology Open Software Suite, *Trends Genet. 16*, 276−277.
29. Levitt, M., and Warshel, A. (1975) Computer simulation of protein folding, *Nature 253*, 694−698.
30. Waterman, M. S., and Eggert, M. (1987) A new algorithm for best subsequence alignments with application to tRNA-rRNA comparisons, *J. Mol. Biol. 197*, 723−728.
31. Huang, X., and Miller, W. (1991) A time-efficient, linar-space local similarity algorithm, *Adv. Appl. Math. 12*, 337−357.
32. Guex, N., and Peitsch, M. C. (1997) SWISS-MODEL and the Swiss-PdbViewer: an environment for comparative protein modeling, *Electrophoresis 18*, 2714−2723.
33. Zeibdawi, A. R., Grundy, J. E., Lasia, B., and Pryzdial, E. L. G. (2004) Coagulation factor Va Glu-96-Asp-111: a chelator-sensitive site involved in function and subunit association, *Biochem. J. 377*, 141−148.
34. Hibbard, L. S., and Mann, K. G. (1980) The calcium-binding properties of bovine factor V, *J. Biol. Chem. 255*, 638−645.
35. Berendsen, H. J. C., van der Spoel, D., and van Drunen, R. (1995) GROMACS: A message-passing parallel molecular dynamics implementation, *Comput. Phys. Commun. 91*, 43−56.
36. Lindahl, E., Hess, B., and van der Spoel, D. (2001) GROMACS 3.0: a package for molecular simulation and trajectory analysis, *J. Mol. Model. 7*, 306−317.
37. van der Spoel, D., van Buuren, A. R., Apol, E., Meulenhoff, P. J., Tieleman, D. P., Sijbers, A. L. T. M., Hess, B., Feenstra, K. A., Lindahl, E., van Drunen, R., and Berendsen, H. J. C. (2002) Gromacs User Manual version 3.1.1, Nijenborgh 4, 9747 AG Groningen, The Netherlands (Internet: http://www.gromacs.org).
38. Jorgensen, W. L., and Madura, J. D. (1985) Temperature and size dependence for Monte Carlo simulations of TIP4P water, *Mol. Phys. 56*, 1381−1392.
39. Jorgensen, W. L., Maxwell, D. S., and Tirado-Rives, J. (1996) Development and testing of the OPLS All-Atom force field on conformational energetics and properties of organic liquids, *J. Am. Chem.* Soc. *118*, 11225−11236.
40. Hess, B., Bekker, H., Berendsen, H. J. C., and Fraaije, J. G. E. M. (1997) LINCS: a linear constraint solver for molecular simulations, *J. Comput. Chem. 18*, 1463−1472.

41. Darden, T., York, D., and Pedersen, L. (1993) Particle mesh Ewald: An N•log(N) method for Ewald sums in large systems, *J. Chem. Phys. 98*, 10089−10092.
42. Essmann, U., Perera, L., Berkowitz, M. L., Darden, T., Lee, H., and Pedersen, L. G. (1995) A smooth particle mesh Ewald method, *J. Chem. Phys. 103*, 8577−8593.
43. Parrinello, M., and Rahman, A. (1980) Structure and pair potentials: a molecular-dynamics study, *Phys. Rev. Lett. 45*, 1196−1199.
44. Åqvist, J. (1990) Ion−water interaction potentials derived from free energy perturbation simulations, *J. Phys. Chem. 94*, 8021−8024.
45. Reichert, D. E., Norrby, P.-O., and Welch, M. J. (2001) Molecular modeling of bifunctional chelate peptide conjugates. 1. Copper and Indium parameters for the AMBER force field, *Inorg. Chem. 40*, 5223−5230.
46. Berendsen, H. J. C., Postma, J. P. M., van Gunsteren, W. F., DiNola, A., and Haak, J. R. (1984) Molecular dynamics with coupling to an external bath, *J. Chem. Phys. 81*, 3684−3690.
47. DeLano, W. L. (2002) Pymol Program, DeLano Scientific, San Carlos, CA.
48. Ramachandran, G. N., Ramakrishnan, C., and Sasisekharan, V. (1963) Stereochemistry of polypeptide chain configurations, *J. Mol. Biol. 7*, 95−99.
49. Kabsch, W., and Sander, C. (1983) Dictionary of protein secondary structure: pattern recognition of hydrogen-bonded and geometrical features, *Biopolymers 22*, 2577−2637.
50. Zaitseva, I., Zaitsev, V., Card, G., Moshkov, K., Bax, B., Ralph, A., and Lindley, P. (1996) The X-ray structure of human serum ceruloplasmin at 3.1 angstrom: Nature of the copper centres, *J. Biol. Inorg. Chem. 1*, 15−23.
51. Berman, H. M., Westbrook, J., Feng, Z., Gilliland, G., Bhat, T. N., Weissig, H., Shindyalov, I. N., and Bourne, P. E. (2000) The Protein Data Bank, *Nucleic Acids Res. 28*, 235−242.
52. Flohil, J. A., Vriend, G., and Berendsen, H. J. C. (2002) Completion and refinement of a 3-D homology models with restricted molecular dynamics: application to targets 47, 58, and 111 in the CASP modeling competition and posterior analysis, *Proteins 48*, 593−604.
53. Pryzdial, E. L., and Mann, K. G. (1991) The association of coagulation factor Xa and factor Va, *J. Biol. Chem. 266*, 8969−8977.
54. Gale, A. J., Xu, X., Pellequer, J. L., Getzoff, E. D., and Griffin, J. H. (2002) Interdomain engineered disulfide bond permitting elucidation of mechanisms of inactivation of coagulation factor Va by activated protein C, *Protein Sci. 11*, 2091−2101.
55. Kalafatis, M., Bertina, R. M., Rand, M. D., and Mann, K. G. (1995) Characterization of the molecular defect in factor VR506Q, *J. Biol. Chem. 270*, 4053−4057.
56. Nicolaes, G. A., Tans, G., Thomassen, M. C., Hemker, H. C., Pabinger, I., Varadi, K., Schwarz, H. P., and Rosing, J. (1995) Peptide bond cleavages and loss of functional activity during inactivation of factor Va and factor VaR506Q by activated protein C, *J. Biol. Chem. 270*, 21158−21166.
57. Heeb, M. J., Kojima, Y., Greengard, J. S., and Griffin, J. H. (1995) Activated protein C resistance: molecular mechanisms based on studies using purified Gln506-factor V, *Blood 85*, 3405−3411.
58. Aparicio, C., and Dahlbäck, B. (1996) Molecular mechanisms of activated protein C resistance. Properties of factor V isolated from an individual with homozygosity for the Arg506 to Gln mutation in the factor V gene, *Biochem. J. 313*, 467−472.
59. Lollar, P., and Parker, C. G. (1990) pH-dependent denaturation of thrombin-activated porcine factor VIII, *J. Biol. Chem. 265*, 1688−1692.
60. Fay, P. J., and Smudzin, T. M. (1992) Characterization of the interaction between the A2 subunit and A1/A3-C1-C2 dimer in human factor VIIIa, *J. Biol. Chem. 267*, 13246−13250.
61. Lu, D., Kalafatis, M., Mann, K. G., and Long, G. L. (1996) Comparison of activated protein C/protein S-mediated inactivation of human factor VIII and factor V, *Blood 87*, 4708−4717.

BI050891T